Acta Agrícola y Pecuaria 12: e0121027. | e-ISSN: 2395-874X.
https://doi.org/10.30973/aap/2026.12.0121027 (June 22th, 2026)

SCIENTIFIC ARTICLE

Evaluation of a low-cost multispectral imaging system for rapid estimation of chemical composition in tropical grasses

Evaluación de un sistema de imagen multiespectral de bajo costo para la estimación rápida de la composición química en pastos tropicales

Julián Arroyave-Jaramillo[1], Daniel M. Pineda-Tobón[2], Luis A. Giraldo-Valderrama[2], Juan C. Pérez-Naranjo[2], Luis Chel-Guerrero[3], David Betancur-Ancona[3]*

[1] Universidad Autonoma de Yucatan, Posgrado Institucional de Ciencias Agropecuarias y Manejo de Recursos Naturales y Tropicales, carretera Merida-Xmatkuil km 15.5, 97315, Merida, Yucatan, Mexico.

[2] Universidad Nacional de Colombia-Sede Medellin, Facultad de Minas, Carretera 80, No- 65-223, 050041, Medellin, Colombia.

[3] Universidad Autonoma de Yucatan, Campus de Ciencias Exactas e Ingenierias, Facultad de Ingenieria Quimica, Periferico Norte km 33.5, Tablaje Catastral 13615, Chuburna de Hidalgo Inn., 97203, Merida, Yucatan, Mexico.

*Corresponding author: bancona@correo.uady.mx

Reception date:
April 29th, 2026

Acceptation date:
May 22th, 2026

Published on line:
June 22th, 2026

How to cite:
Arroyave-Jaramillo, J., Pineda-Tobón, D. M., Giraldo-Valderrama, L. A., Pérez-Naranjo, J. C., Chel-Guerrero, L., Betancur-Ancona, D. (2026). Evaluation of a low-cost multispectral imaging system for rapid estimation of chemical composition in tropical grasses. *Acta AgrícolayPecuaria,12*,e0121027. https://doi.org/10.30973/aap/2026.12.0121027

ABSTRACT

The evaluation of tropical forage nutritional quality using conventional analytical methods is costly and time-consuming, limiting its application in livestock systems. The objective of this work was to develop and validate a low-cost multispectral image spectroscopy system (AFT camera), to estimate the chemical composition of tropical grasses. A total of 332 forage samples, including 293 *Urochloa* spp. and 39 *Megathyrsus maximus* (Jacq.) B.K.Simon & S.W.L.Jacobs, were analyzed using standard laboratory methods and multispectral image regression analysis. Calibration models showed coefficients of determination (R^2) ranging from 0.36 to 0.98, while validation models exceeded 0.60 for neutral detergent fiber and 0.70 for crude protein and digestibility. No significant differences ($p > 0.05$) were detected between observed and predicted values. The AFT system demonstrated potential as a rapid and low-cost tool for forage quality assessment, although calibration performance varied according to forage species and chemical component evaluated.

KEYWORDS

Multispectral spectroscopy, chemical compounds, livestock forage, *Urochloa*, *Megathyrsus*.

RESUMEN

La evaluación de la calidad nutricional de los forrajes tropicales mediante métodos analíticos convencionales es costosa y requiere mucho tiempo, lo que limita su aplicación en los sistemas pecuarios. El objetivo de este trabajo fue desarrollar y validar un sistema de espectroscopia de imágenes multiespectrales de bajo costo (cámara AFT) para estimar la composición química de gramíneas tropicales. Se analizaron 332 muestras de forraje, que incluyeron 293 de *Urochloa* spp. y 39 de *Megathyrsus maximus* (Jacq.) B.K. Simon & S.W.L. Jacobs, mediante métodos convencionales de laboratorio y análisis de regresión a partir de imágenes multiespectrales. Los modelos de calibración mostraron coeficientes de determinación (R^2) 0.36 a 0.98, mientras que los modelos de validación superaron 0.60 para fibra detergente neutro y 0.70 para proteína cruda y digestibilidad. No se detectaron diferencias significativas ($p > 0.05$) entre los valores observados y predichos. El sistema AFT mostró potencial como una herramienta rápida y de bajo costo para la evaluación de la calidad de forrajes, aunque el desempeño de las calibraciones varió según la especie forrajera y el componente químico evaluado.

PALABRAS CLAVE

Espectroscopia multiespectral, compuestos químicos, forraje para ganado, *Urochloa*, *Megathyrsus*.

Introduction

Livestock production in tropical regions faces the challenge of sustainably scaling up to meet the growing demand for animal-based foods, which is projected to increase by more than 40 % by 2050 (Erdaw, 2023). In these systems, pastures constitute more than 70 % of cattle diets, and the nutritional quality of forage is the main determinant of animal productivity (Charmley et al., 2016; Perry et al., 2017). However, routine assessment of forage chemical composition relies on conventional analytical methods that present limitations in terms of cost, time, and accessibility, particularly in developing countries (Jarque-Bascuñana et al., 2021).

Traditional analyses of crude protein (CP), neutral detergent fiber (NDF), acid detergent fiber (ADF), lignin, and digestibility require days of processing, expensive reagents, and trained personnel, limiting their routine application to research or specialized laboratory settings (Dias et al., 2023). This situation restricts evidence-based decision-making for optimizing grazing management, harvest timing, and supplement formulation.

Near-infrared spectroscopy (NIRS) has proven to be an effective alternative for rapid analysis of forage chemical composition (Andueza et al., 2018; Parrini et al., 2018). However, the high cost of commercial equipment remains a limiting factor for its adoption in tropical production systems (Abreu et al., 2023). This limitation has encouraged the development of low-cost optical alternatives based on simplified spectroscopic and imaging approaches.

Multispectral imaging systems integrate principles of spectroscopy and digital image processing, enabling the analysis of chemical properties in plant matrices (Basurto Gutiérrez et al., 2025). Unlike traditional spectrophotometers, multispectral cameras capture two-dimensional spectral information, increasing the representativeness of heterogeneous samples such as forage (Gamon et al., 2019).

Recent studies have explored the use of portable sensors to estimate chemical properties in tropical grasses. Hughes et al. (2017) reported coefficients of determination ranging from 0.23 to 0.65 for digestibility and from 0.08 to 0.79 for ADF in *Urochloa* (formely *Brachiaria*) and *Megathyrsus* species using SPAD (Soil and Plant Analysis Development) chlorophyll meters and NDVI (Normalized Difference Vegetation Index) sensors. These findings suggest the potential of simplified optical technologies; however, the variable accuracy observed indicates the need for more sophisticated systems integrating multiple wavelengths.

This study developed and validated a low-cost multispectral imaging system called the AFT camera to estimate the chemical composition of tropical grasses relevant to Latin American livestock systems. The hypothesis was that integrating spectral information from multiple wavelengths using multivariate statistical models would enable accurate estimation of CP, NDF, ADF, lignin, ash, and *in vitro* dry matter digestibility (IVDMD) in *Urochloa* and *Megathyrsus* species.

Materials and methods

Location

The study was conducted at the Cotove Agricultural Station, Universidad Nacional de Colombia, Medellin Campus (6° 13′ N, 75° 34′ W, 2,470 masl). Climatic conditions during the experimental period included an average temperature of 32 °C, average precipitation of 10 mm/week, and relative humidity of 96 %. Supplementary sprinkler irrigation was applied twice weekly for 20 min, between 8:00 and 9:00 hours.

Plant material and sampling design

Six species of tropical grasses were evaluated: *Urochloa eminii* (Mez) Davidse (formely *Brachiaria decumbens* and *Brachiaria ruziziensis*), *Urochloa dictyoneura* (Fig. & De Not.) Veldkamp (formely *Brachiaria dictyoneura* cv. Llanero and *Brachiaria humidicola*), *Urochloa brizantha* (A.Rich.) R.D.Webster (formely *Brachiaria brizantha* cvs. Marandú, Piata, Xaraes-Toledo), and *Megathyrsus maximus* (Jacq.) B.K.Simon & S.W.L.Jacobs (cvs. Aruana, Massai, Mombaza, Tanzania). Each plot (5 m²) was divided into three sections subjected to initial uniformity cuts at a height of 10 cm. Sections were harvested at 15, 25, and 35 days after regrowth to obtain variability in chemical composition associated with physiological maturity. A total of 332 samples were obtained, of which 293 corresponded to *Urochloa* spp. and 39 to *M. maximus* (Table 1). To improve biological representativeness and reproducibility, each regrowth

Table 1. Distribution of grass samples by species for calibration and validation.

Genus	Species	Calibration	Validation
Urochloa	*Urochloa eminii* (Mez) Davidse cv. 1 (*B. decumbens*)	56	6
	Urochloa eminii (Mez) Davidse cv. 2 (*B. ruziziensis*)	52	6
	Urochloa dictyoneura (Fig. & De Not.) Veldkamp cv. 1 (*B. dictyoneura* cv. Llanero)	36	5
	Urochloa dictyoneura (Fig. & De Not.) Veldkamp cv. 2 (*B. humidicola*)	66	8
	Urochloa brizantha (A.Rich.) R.D.Webster (*B. brizantha* cvs. Marandú, Piata, Xaraes)	16	6
Megathyrsus	*M. maximus* (Jacq.) B.K.Simon & S.W.L.Jacobs (cvs. Aruana, Massai, Mombaza, Tanzania)	53	6

age within each species/cultivar was considered an independent experimental unit. Sampling followed a completely randomized design, and forage material was collected from different sections within each plot to capture intra-plot variability. The distribution of samples among species, cultivars, and regrowth stages was balanced according to field availability. For model development, samples were randomly assigned to calibration (90 %) and external validation (10 %) datasets while maintaining representation of species, cultivar, and regrowth stage within both subsets to minimize selection bias and improve predictive robustness.

Chemical analysis

Samples (~500 g fresh weight) were oven-dried at 60 °C for 48 h (Air drying oven, Gylson Company Inc, Delaware OH, USA), ground using a hammer mill (Buhler, Alzenau, Germany) and sieved to 1 mm. Chemical analyses followed standardized methods. Nitrogen was determined using a Kjeltec system, and crude protein (CP) was calculated as N × 6.25 according to AOAC method 954.01 (Latimer, 2023). Neutral detergent fiber (NDF), acid detergent fiber (ADF), and lignin were quantified using the sequential method of Van Soest et al. (1991) with an ANKOM 200® fiber analyzer (ANKOM Technology, New York, USA). Ash content was determined by calcination at 550 °C for 4 h (AOAC method 923.03). *In vitro* dry matter digestibility (IVDMD) was measured after 48 h incubation at 40 °C using an ANKOM Daisy II incubator system (ANKOM Technology, New York, USA) and ruminal fluid collected from Holstein cows fed a diet consisting of *Cenchrus clandestinus* (Hochst. ex Chiov.) Morrone (90 %) and commercial concentrate (10 %), following Cabral et al. (2020). All analyses were performed in triplicate (n = 3) and expressed on a dry basis (% db).

AFT multispectral imaging system

The AFT system consists of an integrating hemisphere with a radius of 15 cm, equipped with an LED lighting module, a 2 MP webcam (Shenzhen Weinan Electronic Co., Ltd. China) with the infrared filter removed, an electronic control circuit, and an Arduino UNO board (Advanced Technology S.A., Medellin, Colombia). The LED module included narrow-band LEDs covering the visible and near-infrared regions was operated under controlled current conditions to ensure stable light intensity during image acquisition. The integrating hemisphere minimized directional reflection and reduced illumination heterogeneity across the sample surface. Image acquisition was performed in a closed chamber under constant environmental conditions to avoid interference from external light sources (Figure 1). The control software was developed in Python 3.6. The operating principle was based on diffuse reflectance: each sample was illuminated sequentially with 17 wavelengths (Table 2), capturing images with equidistant triangular geometry over a sampling area of 7 cm^2.

Samples were placed in a cylindrical sample holder (3.5 cm^3) with a leveled surface. Image acquisition generated 17 sequential 8-bit grayscale images (0-255, where 0 = black and 255 = white). Image processing was conducted using a macro developed in ImageJ 1.52 (Schindelin et al. 2015), extracting the average value from the central region of interest (75 × 75 pixels). Prior to data acquisition, the system was calibrated using a diffuse white reflectance reference

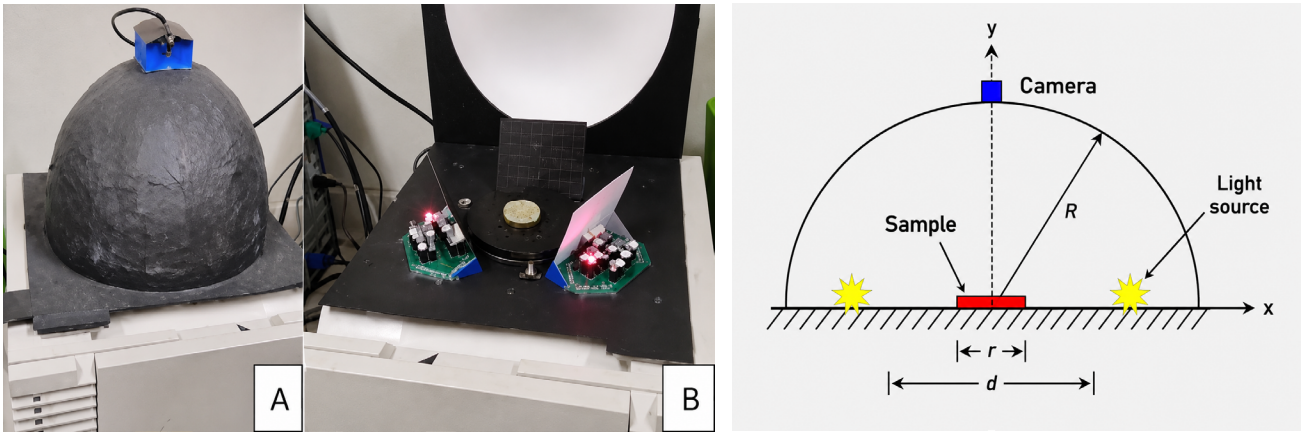

Figure 1. AFT systems for estimating the chemical composition of tropical grasses. (A) Light integrating hemisphere. (B) Location lighting system of the camera and sample. R = radius of the integrating hemisphere to distribute light evenly over the sample, d = center of the coordinate axis for placing the LEDs in a triangular pattern and equidistant from each other, r = radius of the sampling area (1.5 cm).

Table 2. Wavelengths of the AFT camera's LED lighting system.

LED	Wavelength (nm)	Spectral region	Spectral region
1-3	428	Visible-blue	Chlorophyll b absorption
4-6	445	Visible-blue	Chlorophyll b absorption
7-9	465	Visible-blue	Transition Blue-green
10-12	493	Visible-green	Reflectance of vegetation
13-15	525	Visible-green	Reflectance of vegetation
16-18	560	Visible-yellow-green	Carotenoid absorption
19-21	590	Visible-yellow	Transition yellow-red
22-24	607	Visible-orange	Chlorophyll a pre-absorption
25-27	630	Visible-red	Chlorophyll a absorption
28-30	650	Visible-red	Maximum chlorophyll a absorption
31-33	730	Red edge	Transition visible-NIR
34-36	780	Close to NIR	Cellular structure
37-39	840	NIR	NDVI index
40-42	850	NIR	Foliar dispersion
43-45	870	NIR	Water content
46-48	910	NIR	O-H, N-H vibrations
49-51	940	NIR	Water absorption

NIR = near infrared.

standard to normalize illumination conditions among measurements. The central region of interest was selected to avoid edge effects, shadows, and non-uniform particle distribution, thereby improving signal stability and repeatability.

Statistical analysis

The analyses were performed in R 3.6.1 (R Core Team, 2019) using the packages *leaps* for regression analysis, *corrplot* for correlational analysis, and *agricolae* for mean comparisons. Ninety percent of the samples were assigned to calibration, with 10 % were reserved for external validation. Multiple linear regression models were developed for each analyzed component using bidirectional stepwise selection based on the Akaike information criterion (AIC), with the 17 gray values used as independent variables according to:

$$Y = \beta_0 + \beta_1 X_1 + \beta_2 X_2 + \ldots + \beta_{17} X_{17} + \varepsilon$$

Where Y represents the component, X_1-X_{17} are grayscale values at each wavelength, β_0-β_{17} are regression coefficients, and ε is the residual error.

Because the number of spectral predictors could increase the risk of overfitting in reduced datasets, model performance was evaluated not only through calibration statistics but also using external validation metrics and residual analysis. The behavior of residual distribution, prediction bias, and homoscedasticity were examined to assess model stability and predictive reliability.

For calibration, the coefficient of determination (R^2) and mean square error (MSE) were calculated, whereas validation included R^2p, standard error of prediction (SEP), and root mean square error of prediction (RMSEP). Analysis of variance (ANOVA) was used to compare reference and predicted values for each chemical component and species ($p < 0.05$). For *B. ruziziensis*, partial least squares (PLS) regression with cross-validation was additionally evaluated following the standard NIRS approach (Abreu et al., 2023; Monrroy et al., 2017). PLS analysis was performed in JMP Pro 15 using the NIPALS algorithm (JMP Statistical Discovery LLC, North Caroline, USA) with leave-one-out cross-validation (K = 32). Calibration R^2, cumulative Q^2, and RMSECV were calculated and compared with stepwise regression to assess model robustness. The inclusion of both stepwise regression and PLS approaches allowed comparison between an interpretable variable-selection strategy and a multivariate latent-variable method commonly applied in spectroscopic prediction models (Abreu et al., 2023).

Results and discussion

Chemical composition of grasses

Table 3 shows the chemical composition of the six forage materials evaluated. NDF values ranged from 63.54 % in *Urochloa eminii* (Mez) Davidse cv.2 (*B. ruziziensis*) to 70.01 % in *Urochloa dictyoneura* (Fig. & De Not.) Veldkam cv.1 (*B. dictyoneura*), with wide within-species variation (48.49-80.54 %), reflecting the effect of regrowth age. Mean ADF content ranged from 28.04 % in *Urochloa eminii* (Mez) Davidse cv. 1 (*B. decumbens*) to 33.12 % in *Urochloa dictyoneura* (Fig. & De Not.) Veldkam cv.1 (*B. dictyoneura*). Lignin concentrations varied from 3.35 % to 3.96 % and exhibited high coefficients of variation (11.47-33.79 %), indicating sensitivity to physiological maturity. CP content was higher in *Urochloa eminii* (Mez) Davidse cv. 1 (*B. decumbens*) with 17.41 %, exceeding the values observed in the remaining species (12.10-15.36 %). IVDMD ranged from 50.63 % in *Urochloa brizantha* (A.Rich.) R.D.Webster (*B. brizantha*) to 60.76 % in *Urochloa eminii* (Mez) Davidse cv. 1 (*B. decumbens*), with broad variation (35.77-74.25 %), reflecting the greater digestibility of younger plant material.

Table 3. Chemical composition and *in vitro* digestibility of tropical grasses (% db).

Species	Statistical	NDF	ADF	Lignin	Ash	CP	IVDMD
Urochloa brizantha (*B. brizantha*)	Mean ± SD	67.24 ± 4.11	31.54 ± 3.23	3.83 ± 0.70	7.44 ± 3.96	12.60 ± 2.80	50.63 ± 5.36
	Range	57.93-78.20	23.26-40.78	2.87-6.73	2.53-12.97	8.01-19.48	35.77-59.55
Urochloa dictyoneura cv.1 (*B. dictyoneura*)	Mean ± SD	70.01 ± 3.56	33.12 ± 2.78	3.35 ± 0.38	6.30 ± 3.81	12.10 ± 2.73	55.51 ± 6.53
	Range	59.80-76.26	25.27-36.68	2.57-4.34	2.25-13.48	8.45-20.58	42.48-67.79
Urochloa eminii cv. 1 (*B. decumbens*)	Mean ± SD	64.36 ± 5.19	28.04 ± 4.57	3.58 ± 1.21	5.79 ± 3.79	17.41 ± 5.03	60.76 ± 7.82
	Range	51.36-80.54	18.83-40.49	1.92-6.78	2.16-13.01	5.63-24.64	44.57-74.25
Urochloa eminii cv. 2 (*B. ruziziensis*)	Mean ± SD	63.54 ± 5.70	29.48 ± 4.45	3.90 ± 0.76	7.58 ± 4.42	14.08 ± 3.18	51.98 ± 5.51
	Range	48.49-74.14	19.07-36.36	2.77-6.99	1.83-14.56	9.08-22.45	44.15-68.18
Urochloa dictyoneura cv. 2 (*B. humidicola*)	Mean ± SD	65.90 ± 4.80	30.45 ± 3.38	3.96 ± 1.09	5.29 ± 3.39	14.83 ± 2.93	56.70 ± 6.75
	Range	52.57-79.14	21.31-39.36	2.38-7.33	2.43-14.64	8.09-23.03	41.09-68.58
Megathyrsus maximus	Mean ± SD	67.61 ± 4.90	31.98 ± 4.29	3.76 ± 0.61	2.84 ± 0.25	15.36 ± 3.08	52.53 ± 9.07
	Range	56.68-76.58	24.71-41.58	2.44-5.17	2.16-3.26	9.14-21.92	38.62-73.22

NDF = neutral detergent fiber (%); ADF = acid detergent fiber (%); CP = crude protein (%); IVDMD = *in vitro* dry matter digestibility (%); SD = standard deviation.

These values are consistent with those reported by Torres-Lugo et al. (2022) for the ecotypes *Urochloa* Mulato II, Cayman, Talisman Camello, Marandu, and *M. maximus* cv. Mombasa, which exhibited CP, NDF, and ADF values ranging from 10-15 %, 59-67 %, and 35-40 %, respectively. In *Urochloa eminii* cv. 2 (*Brachiaria ruziziensis*), chemical composition has been shown to vary with harvest age, with CP ranging from 2.3 % to 7.3 %, ash from 8 % to 14 %, NDF from 62 % to 66 %, ADF from 46 % to 52 %, and IVDMD 48 % to 54 % (Ariyo et al., 2025), supporting the representativeness of the calibration dataset used in the present study. The three-stage regrowth harvesting strategy generated substantial compositional variability, a key requirement for the development of robust spectroscopic predictive models (Jarque-Bascuñana et al., 2021). The observed ranges exceed the variability typically found under uniform commercial management, thereby enhancing the predictive capacity of the models under diverse practical conditions.

Calibration model performance

The coefficients of determination (R^2) between gray-scale values and forage chemical composition varied considerably among species and analytes (Table 4). *Urochloa brizantha* (*B. brizantha*) and *Urochloa dictyoneura* cv.1 (*B. dictyoneura*) exhibited the best overall model performance, with R^2 values exceeding 0.80 for all analytes. In *Urochloa brizantha*, R^2 reached 0.96 for lignin, 0.95 for ADF, 0.92 for NDF, 0.94 for ash, 0.91 for CP, and 0.92 for IVDMD. Similarly, *Urochloa dictyoneura* cv.1 (*B. dictyoneura*) achieved R^2 values of 0.95 for lignin, 0.91 for ADF, 0.82 for NDF, 0.81 for ash, 0.84 for CP, and 0.83 for IVDMD.

The remaining species exhibited moderate to low predictive performance for certain components. Generally, *Urochloa dictyoneura* cv. 2 (*B. humidicola*) showed the lowest R^2 values (0.35-0.63). Notably, *Urochloa eminii* cv. 1 (*B. decumbens*) exhibited excellent predictive performance for CP (R^2 = 0.96), whereas the model fit for IVDMD was more moderate (R^2 = 0.56). Ash content generally showed the weakest model performance across species, possibly due to variability associated with contamination by mineral particles during manual harvesting. These results indicate that spectral information provided by the 17 selected wavelengths effectively captured compositional variability, consistent with the physicochemical principles governing light-matter interactions. In the visible region (428-650 nm), differential absorption by chlorophylls and carotenoids is indirectly correlated with leaf protein concentration. Approximately 50-70 % of foliar nitrogen is located within chloroplasts, primarily in proteins involved in the photosynthetic apparatus (Luo et al., 2021). The AFT bands centered at 428 nm, 445 nm, 630 nm, and 650 nm correspond to chlorophyll absorption regions, which likely explains the high R^2 values obtained for CP prediction.

In the near infrared region (780-940 nm), reflectance is largely governed by multiple scattering within the leaf mesophyll and is proportional to the volume of intercellular spaces. Progressive lignification during plant maturation reduces air spaces, resulting in lower NIR reflectance (Robles-Zazueta et al., 2022). This relationship may explain the moderate to high R^2 values for NDF, ADF, and lignin predictions.

Validation of predictive models

The validation parameters are shown in Table 5. The predictive performance of the models dependent on both species and analyte, and the prediction coefficients of determination (R^2p) varied considerably among

Table 4. Coefficients of determination (R^2) of calibration models for chemical components and digestibility of tropical grasses.

Species	NDF	ADF	Lignin	Ash	CP	IVDMD
Urochloa brizantha (*B. brizantha*)	0.92	0.95	0.96	0.94	0.91	0.92
Urochloa dictyoneura cv.1 (*B. dictyoneura*)	0.82	0.91	0.95	0.81	0.84	0.83
Urochloa eminii cv. 1 (*B. decumbens*)	0.69	0.87	0.59	0.43	0.96	0.56
Urochloa eminii cv. 2 (*B. ruziziensis*)	0.66	0.59	0.86	0.51	0.74	0.68
Urochloa dictyoneura cv. 2 (*B. humidicola*)	0.63	0.61	0.60	0.35	0.63	0.55
Megathyrsus maximus	0.74	0.76	0.58	0.43	0.66	0.74

NDF = neutral detergent fiber; ADF = acid detergent fiber; CP = crude protein; IVDMD = *in vitro* dry matter digestibility (%).

species and analytes (Figure 2). For NDF, five species achieved R^2p values greater than 0.60 (*M. maximus*, 0.85; *U. dictyoneura* cv. 1, 0.78; *U. brizantha* 0.68; *U. eminii* cv. 1, 0.68; and *U. eminii* cv. 2, 0.65), whereas *U. dictyoneura* cv. 2 exhibited a substantially lower value (0.19). For ADF, four species achieved R^2p values exceeding 0.80 (*U. dictyoneura* cv. 1, 0.98; *U. brizantha* 0.88; *U. eminii* cv. 1, 0.89; *M. maximus*, 0.83). CP content showed R^2p values above 0.70 in five species, except *B. humidicola* (0.38). IVDMD exhibited the highest overall predictive performance, with R^2p values greater than 0.70 in four species (*U. dictyoneura* cv. 1, 0.98; *U. brizantha*, 0.82; *M. maximus*, 0.78; *U. eminii* cv. 1, 0.74). RMSEP values were consistently lower for lignin (0.25-1.09) and ash (0.20-2.75) than for NDF (1.38-4.01), ADF (0.61-2.95), and IVDMD (1.05-8.56). *Urochloa dictyoneura* cv. 2 (*Brachiaria humidicola*) exhibited the highest RMSEP values for several components, consistent with its low R^2p values. For IVDMD, the validation RMSEP reached 8.56 %, compared with a calibration error of 1.30 %, indicating possible overfitting for this component in this species. This limitation is further supported by the low R^2p value observed for lignin (0.36) in the same species, suggesting that an increased sample size will be required in future calibrations. Stepwise selection with AIC reduced the number of active predictors in the models, partially mitigating this risk. However, with a sample size of only n = 16, this approach is insufficient to ensure robust model generalization across all analytes.

The results revealed two distinct groups of components: those with consistently high predictive performance across most species (ADF, PC, IVDMD, with $R^2p > 0.70$ in at least four of six species evaluated); and those showing variable or limited performance that would benefit from additional calibration efforts (lignin in *Urochloa dictyoneura* cv.1 and *Urochloa brizantha*, ash in several species, and all analytes in *Urochloa dictyoneura* cv. 2).

Statistical comparison between methods

Table 6 presents the comparison between reference values and predictions generated by the AFT camera. No statistically significant differences ($p > 0.05$) were detected in 96.7 % of the comparisons (35 out of 36 cases). The only exception was lignin content in *Urochloa dictyoneura* cv. 2 (*B. humidicola*, $p = 0.02$), for which the predicted values underestimated the reference values

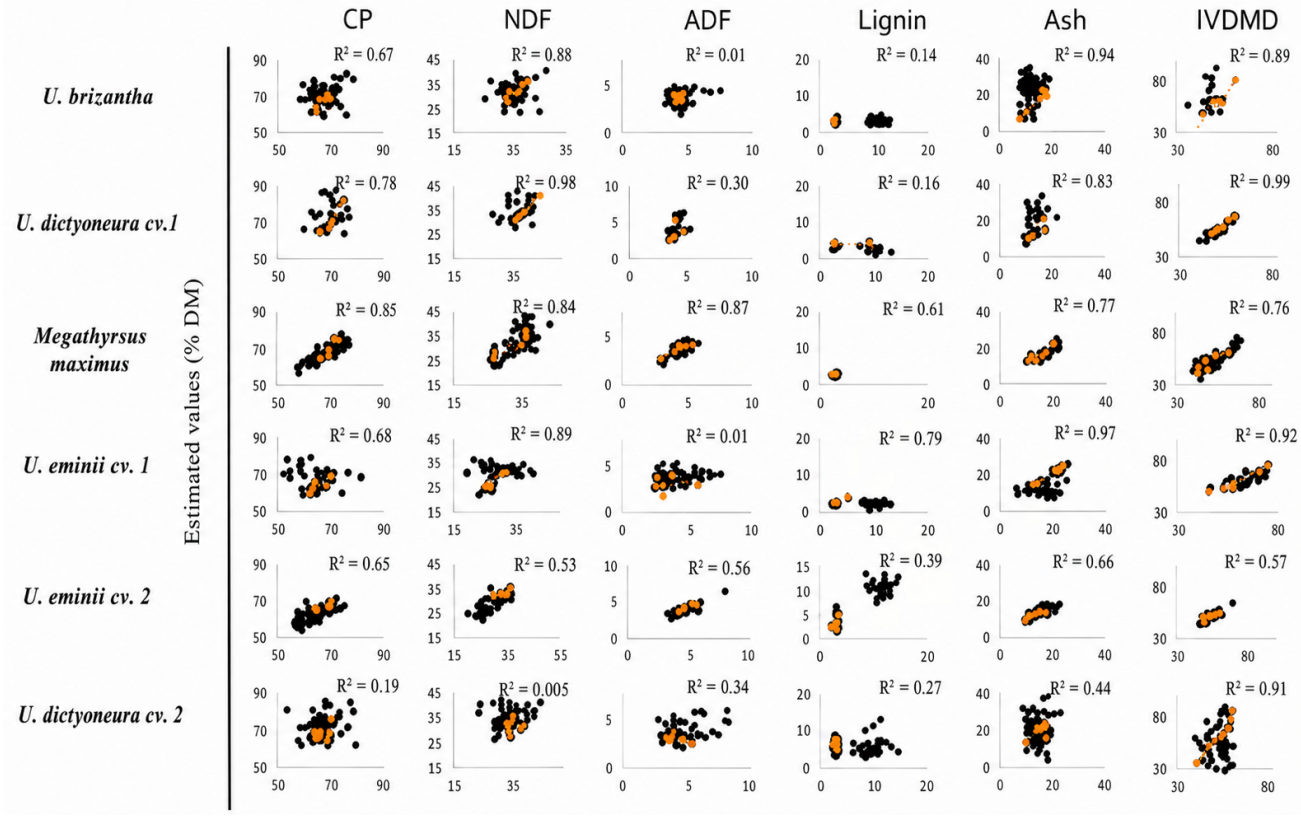

Figure 2. Prediction correlation coefficients (R^2p). Black: data used for model construction, orange: data used in model validation.

Table 5. Validation parameters for predictive models for chemical components and digestibility of tropical grasses.

Species	Component	n value	R^2p	RMSEP	SEP
Megathyrsus maximus	NDF	6	0.85	2.24	2.45
	ADF	6	0.83	1.70	1.86
	Lignin	6	0.84	0.29	0.32
	Ash	6	0.61	0.20	0.22
	CP	6	0.71	1.59	1.74
	IVDMD	5	0.78	3.95	4.33
Urochloa brizantha (*B. brizantha*)	NDF	5	0.68	1.95	2.14
	ADF	5	0.88	1.02	1.12
	Lignin	5	0.36	0.33	0.36
	Ash	5	0.52	0.52	0.57
	CP	5	0.81	2.00	2.19
	IVDMD	8	0.82	8.56	9.38
Urochloa dictyoneura cv.1 (*B. dictyoneura*)	NDF	8	0.78	3.79	4.24
	ADF	8	0.98	1.10	1.23
	Lignin	8	0.22	0.77	0.86
	Ash	8	0.41	2.75	3.07
	CP	8	0.78	2.00	2.24
	IVDMD	6	0.98	1.05	1.17
Urochloa dictyoneura cv. 2 (*B. humidicola*)	NDF	6	0.19	4.01	4.29
	ADF	6	0.47	2.95	3.15
	Lignin	6	0.31	1.05	1.12
	Ash	6	0.48	0.69	0.74
	CP	6	0.38	3.86	4.13
	IVDMD	6	0.69	7.20	7.70
Urochloa eminii cv. 2 (*B. ruziziensis*)	NDF	6	0.65	1.38	1.51
	ADF	6	0.53	1.67	1.83
	Lignin	6	0.55	0.25	0.27
	Ash	6	0.44	0.76	0.83
	CP	6	0.75	1.63	1.79
	IVDMD	6	0.57	2.93	3.21
Urochloa eminii cv. 1 (*B. decumbens*)	NDF	6	0.68	1.82	1.99
	ADF	6	0.89	0.61	0.67
	Lignin	6	0.28	1.09	1.19
	Ash	6	0.79	0.37	0.41
	CP	6	0.92	0.72	0.79
	IVDMD	6	0.74	3.01	3.30

R^2p = coefficient of determination of prediction; RMSEP = root mean square error prediction; SEP = standard error of prediction. SEP = RMSEP × $\sqrt{(n/(n-1))}$.

Table 6. Statistical comparison between measured and predicted values with the AFT camera.

Species	Component	Analytic determination	Measurement AFT camera	*p*-value
Urochloa eminii cv. 1 (*B. decumbens*)	CP	19.13	19.12	0.99
	NDF	64.35	64.37	0.95
	ADF	27.53	27.50	0.96
	Lignin	3.08	3.06	0.97
	Ash	3.22	3.21	0.99
	IVDMD	59.30	59.32	0.84
Urochloa dictyoneura cv.1 (*B. dictyoneura*)	CP	13.26	13.28	0.99
	NDF	70.04	70.06	0.96
	ADF	34.25	34.26	0.98
	Lignin	3.26	3.27	0.99
	Ash	3.95	3.96	0.99
	IVDMD	59.58	59.53	0.99
Urochloa brizantha (*B. brizantha*)	CP	15.41	15.42	0.95
	NDF	66.84	66.83	0.98
	ADF	31.79	31.72	0.99
	Lignin	3.84	3.83	0.96
	Ash	2.85	2.85	0.99
	IVDMD	54.81	54.85	0.99
Urochloa dictyoneura cv. 2 (*B. humidicola*)	CP	15.40	18.39	0.07
	NDF	66.31	68.70	0.14
	ADF	31.46	31.64	0.87
	Lignin	3.77	3.13*	0.02
	Ash	3.01	3.29	0.18
	IVDMD	59.86	63.55	0.57
Urochloa eminii cv. 2 (*B. ruziziensis*)	CP	12.65	12.68	0.96
	NDF	66.70	66.68	0.99
	ADF	33.40	33.83	0.98
	Lignin	4.40	4.42	0.89
	Ash	2.82	2.80	0.97
	IVDMD	51.58	51.58	0.99
Megathyrsus maximus	CP	15.00	15.01	0.99
	NDF	69.26	69.36	0.97
	ADF	31.83	31.85	0.99
	Lignin	3.85	3.87	0.96
	Ash	2.68	2.70	0.91
	IVDMD	50.78	50.80	0.99

*Significant difference $p < 0.05$.

(3.13 % vs. 3.77 %, respectively). For CP, the predicted values showed excellent agreement with the reference measurements, with absolute differences of less than 0.03 percentage points in five species. For NDF, deviations were generally below 0.5 %, except in *U. dictyoneura* cv. 2 (2.4 %), although this difference was not statistically significant. Cell wall constituents (ADF, and lignin) also exhibited high agreement between methods, with mean differences below 0.2 % for ADF and below 0.1 % for lignin, excluding *U. dictyoneura* cv. 2.

The absence of significant differences between AFT predictions and reference measurements in 96.7 % of cases validates the accuracy of the system for nutritional assessment and decision-making. Differences below 1 % for CP, NDF, and ADF were within the expected intralaboratory analytical variability of the reference methods described by Van Soest et al. (1991), indicating that the AFT system provides nutritionally equivalent information to that obtained through conventional laboratory analyses.

Methodological comparison: PLS vs. stepwise regression in *Urochloa eminii* cv. 2 (*B. ruziziensis*)

Table 7 compares the performance of PLS with cross-validation and stepwise regression with holdout validation for *Urochloa eminii* cv. 2. The PLS models identified two latent factors explaining 47-84 % of the variance in the evaluated analytes. For NDF, PLS showed superior calibration (R^2 = 0.84 vs. 0.66) with Q^2 = 0.58 and similar prediction error (RMSECV = 1.43 % vs. RMSEP = 1.38 %). Lignin showed the highest predictive capacity in the PLS models (Q^2 = 0.71; R^2 = 0.75), although stepwise regression yielded a lower prediction error. CP and ADF exhibited moderate predictive performance in both approaches, whereas ash and IVDMD were predicted less accurately (R^2 < 0.51), likely reflecting their greater intrinsic variability. PLS provided a more parsimonious modeling framework by reducing the original set of correlated spectral variables to two latent factors, an important advantage when dealing with multicollinearity in spectral databases. Both methods identified NDF and lignin as best-estimated components. For small datasets (n < 50), PLS maximizes efficiency (Jarque-Bascuñana et al., 2021; Parrini et al., 2018); for larger datasets (n > 100), stepwise improves interpretability. Results agree with NIRS calibrations for *Urochloa* spp. (formerly *Brachiaria* spp). (Monrroy et al., 2017) using NIRS (R^2 = 0.87 for NDF, 0.88 for ADF), validating that the AFT system achieves performance comparable to commercial equipment.

The performance of the AFT system must be contextualized in relation to established forage analysis technologies. For example, Monrroy et al. (2017) calibrated NIRS models for *Urochloa* spp. reporting R^2 of 0.87 for NDF, 0.88 for ADF, with PLS, values comparable

Table 7. Statistical comparison between PLS with cross-validation and stepwise regression with holdout validation for *Urochloa eminii* cv. 2 (*B. ruziziensis*) as a methodological model.

Component	Method	No factors / variables	R^2 Calibration	RMSECV/ RMSEP	Q^2
CP	PLS	2	0.51	2.13	0.55
	Stepwise	17	0.74	1.63	-
NDF	PLS	2	0.84	1.43	0.58
	Stepwise	17	0.66	1.38	-
ADF	PLS	2	0.59	2.85	0.43
	Stepwise	17	0.59	1.67	-
Lignin	PLS	2	0.75	0.38	0.71
	Stepwise	17	0.86	0.25	-
Ash	PLS	2	0.47	3.22	0.27
	Stepwise	17	0.51	0.76	-
IVDMD	PLS	2	0.51	3.86	0.51
	Stepwise	17	0.68	2.93	-

PLS = partial least squares regression; R^2 = coefficient of determination; Q^2 = cross-validation prediction coefficient; RMSECV = root mean square error of cross-validation; RMSEP = root mean square error of prediction; CP = crude protein (%); NDF = neutral detergent fiber (%); ADF = acid detergent fiber (%); IVDMD = *in vitro* dry matter digestibility (%).

to those obtained with the AFT system for *Urochloa eminii* cv. 2 (*B. ruziziensis*) (R^2 = 0.84 for NDF with PLS; Table 7), and 0.65 (CP), with RMSEPs of 1.71 %, 1.36 %, and 0.71%, respectively. Likewise, the RMSEP values obtained with the AFT system for *U. brizantha* (NDF 1.95 %, ADF 1.02 %) and *Urochloa eminii* cv. 2 (*B. ruziziensis*) (NDF 1.38 %) were within the range reported for NIRS. Notably, the R^2p values obtained for CP (0.71-0.92) consistently exceeded those reported with NIRS, possibly due to greater emphasis on chlorophyll-sensitive visible bands in the AFT design.

Thomson et al. (2018) used NIRS to be mixed forages samples and obtained R^2 values ranging from 0.76-0.91, with standard calibration errors of 13.4 % for NDF and 18.5 % for ADF. In comparison, the SEP values obtained with the AFT system were generally lower (3.07-17.98 % for NDF and 0.83-6.77 % for ADF), suggesting that the multispectral AFT approach efficiently captures variability in tropical forages. Hughes et al. (2017) reported considerably lower predictive performance using a SPAD-502 meter, with R^2 values ranging from 0.08 to 0.34 for ADF and from 0.14 to 0.31 for NDF in *Urochloa* (*Brachiaria*) and *Megathyrsus*. These values were substantially lower than those achieved with the AFT system (0.59-0.95 for ADF, 0.63-0.92 for NDF). Using the NDVI meter, the same authors obtained R^2 values of 0.54-0.79 for ADF, which also remained below the best results obtained with the AFT system. The principal advantage of the developed system lies in its acquisition of multidimensional spectral information across 17 bands, compared with the limited spectral information provided by conventional biosensors, thereby enabling more robust predictive modeling.

Variability between species and spectroscopic fundamentals

The variability in model performance among species (*U. dictyoneura* cv. 2 R^2 = 0.35-0.63 vs. *U. brizantha* = 0.91-0.96) may be attributed to differences in leaf optical properties that influence reflectance independently of chemical composition. *Urochloa dictyoneura* cv. 2 (*B. humidicola*) is characterized by dense leaf pubescence and prominent epicuticular waxes (Namazzi et al., 2020) that could have increased specular scattering, reducing compositional information in a captured diffuse signal. Previous research has shown that leaf trichomes increase reflectance within 400-700 nm range by 15-30 %, partially masking absorption by photosynthetic pigments (Xiong et al., 2015).

The stratification of models by species vs. universal model significantly improved performance in preliminary calibrations, confirming that species-specific optical characteristics justify independent calibrations. This approach is consistent with NIRS practices, where universal equations present errors greater than specific calibrations (Abreu et al., 2023). The lower predictive performance observed for ash content (*U. dictyoneura* cv. 2, R^2 = 0.35, *M. maximus*, R^2 = 0.43) probably reflects variability associated with mineral contamination during manual harvesting rather than differences in intrinsic mineral composition. Minerals generally lack distinctive spectral features within 400-1,000 nm range, limiting their direct prediction through reflectance spectroscopy (Ancin-Murguzur et al., 2020). Consequently, the implementation of improved sampling protocols, including controlled mechanical harvesting, could help reduce this source of variability and enhance model performance.

Operational advantages and practical applicability

Among the advantages of the AFT camera, the analysis time of ~5 min from sample insertion to result generation was particularly noteworthy, representing a reduction of more than 95 % compared with conventional laboratory methods, which typically require 2-5 days when drying, grinding, and chemical analysis are considered. This rapid feedback would enable adjustments to grazing management, harvest optimization, supplement formulation, and critical applications in precision livestock farming (Kleen & Guatteo, 2023). Furthermore, the estimated cost of the AFT system components (< USD 500) is substantially lower than that of commercial NIRS equipment (USD 40,000-100,000) and automated fiber analyzers (USD 15,000-30,000). This favorable cost-to-benefit ratio democratizes access to forage analysis for small and medium-scale producers in tropical regions, who often lack access to affordable analytical services (Fakude et al. 2025).

Operation of the system does not require hazardous reagents or generate chemical waste, thereby reducing environmental impacts and eliminating many of the recurring costs associated with con-

ventional laboratory analyses. The only preparation required involves operations such as drying and grinding, which are generally standardized for sample preparation and preservation, so no further complexity is required.

Implications for sustainable tropical livestock farming

Sustainable intensification of tropical livestock farming requires improving forage-to-animal conversion efficiency while minimizing environmental impacts (Erdaw, 2023). Affordable tools such as the AFT camera can support evidence-based decision-making by optimizing harvest timing to balance forage yield and nutritional quality (Caradus & Chapman, 2024), adjusting supplementation through accurate protein and energy assessment (Tan et al., 2021), and facilitating the selection of forage species adapted to local environmental conditions (Rao et al., 2015). It may also enable early detection of pasture degradation associated with overgrazing, enabling timely corrective actions (Costa et al., 2021). By reducing the economic and technical barriers to forage analysis using technologies such as the AFT camera, directly contributing to Sustainable Development Goals related to food security and rural development in tropical regions (Ghosh & Sahu, 2023). Future improvements may include extending the spectral range to 950-1100 nm, integration of advanced machine-learning algorithms (Paul et al., 2025), transferable calibrations (Zhao et al., 2019), and miniaturization with GPS-enabled field monitoring (Radočaj et al., 2023).

Conclusions

The AFT multispectral imaging system demonstrated a consistent capacity to estimate the chemical composition of tropical forage grasses with moderate to high predictive accuracy (R^2p = 0.35-0.98), highlighting its potential as a rapid and low-cost alternative to conventional laboratory analyses. The best predictive performance was observed for crude protein and *in vitro* dry matter digestibility, whereas ash content and some fiber fractions exhibited lower predictive accuracy. Comparison between stepwise regression and PLS regression was performed only for *Urochloa eminii* cv. 2 (*B. ruziziensis*), where PLS showed improved prediction for neutral detergent fiber, achieving performance comparable to values reported for some NIRS-based applications. However, these results should be interpreted specifically for this species and not generalized to the entire AFT system.

Predictive performance varied among species, with *Urochloa brizantha* (*B. brizantha*) and *Urochloa dictyoneura* cv.1 (*B. dictyoneura*) showing the most robust results (R^2 > 0.80), while *Urochloa dictyoneura* cv. 2 (*B. humidicola*) was affected by surface optical properties. *Urochloa dictyoneura* cv. 2 showed the lowest performance in several components, and that IVDMD in *U. brizantha* requires additional calibrations with a larger number of samples before its practical applications.

The absence of significant differences between reference and predicted values in most comparisons supports the practical applicability of the AFT system for forage quality assessment. Overall combination of rapid analysis, low operational cost, and satisfactory predictive performance suggest that multispectral imaging represents a promising tool for supporting nutritional management and decision-making in tropical livestock production systems.

Acknowledgements

The authors would like to thank the Secretaría de Ciencia, Humanidades, Tecnología e Innovación for its financial support during the development of this project. To the Government of Antioquia (Colombia) for partial funding (Agreement No. 4600007658). To the BIORUM Laboratory (Universidad Nacional de Colombia) for providing equipment for chemical analysis.

Literature cited

Abreu, L. F., Lana, Â. M. Q., Climaco, L. C., Matrangolo, W. J. R., Barbosa, E. P., Da Silva, K. T., Rowntree, J. E., Da Silva, E. A., & Simeone, M. L. F. (2023). Near-infrared spectroscopy and chemometrics methods to predict the chemical composition of *Cratylia argentea*. *Agronomy, 13*(10), 2525. https://doi.org/10.3390/agronomy13102525

Ancin-Murguzur, F. J., Brown, A. G., Clarke, C., Sjøgren, P., Svendsen, J. I., & Alsos, I. G. (2020). How well can near infrared reflectance spectroscopy (NIRS) mea-

sure sediment organic matter in multiple lakes? *Journal of Paleolimnology, 64*, 59-69. https://doi.org/10.1007/s10933-020-00121-5

Andueza, D., Picard, F., Dozias, D., & Aufrère, J. (2018). Fecal near-infrared reflectance spectroscopy prediction of the feed value of temperate forages for ruminants and some parameters of the chemical composition of feces: Efficiency of four calibration strategies. *Applied Spectroscopy, 71*(9), 2164-2176. https://doi.org/10.1177/0003702817712740

Ariyo, S. O., Adeyemi, A. A., Adewale, A. S., Alao, O. J., Aderemi, O. V. O., Sadiat, A. A., & Esther, O. T. (2025). Interactive effects of nitrogen fertilization and harvest age on the nutritional composition of *Brachiaria ruziziensis*. *Journal of Soil Plant and Environment, 4*(2), 1-17. https://doi.org/10.56946/jspae.v4i2.661

Basurto Gutiérrez, R., Ramírez Rodríguez, E., & Mariscal Landín, G. (2025). Estimación de la composición química de granos y pastas proteicas mediante espectroscopia (NIRS-FTIR). *Revista Mexicana de Ciencias Pecuarias, 16*(2), 428-445. https://doi.org/10.22319/rmcp.v16i2.6637

Cabral, Í. dos S., Oliveira, S. S., Azevêdo, J. A. G., Souza, L. L., De Lima, R. F., Lopes, C. da C., Otani, F. S., Reis, S. M., & Sousa, C. A. F. (2020). Ruminal fermentation kinetics of by-products using the semi-automatic technique of *in-vitro* gas production. *Revista Brasileira de Saúde e Produção Animal, 21*(01-08), e2121242020, https://doi.org/10.1590/s1519-99402121242020

Caradus, J. R., & Chapman, D. F. (2024). Evaluating pasture forage plant breeding achievements: a review. *New Zealand Journal of Agricultural Research, 68*(6), 1146-1220. https://doi.org/10.1080/00288233.2024.2395370

Charmley, E., Williams, S. R. O., Moate, P. J., Hegarty, R. S., Herd, R. M., Oddy, V. H., Reyenga, P., Staunton, K. M., Anderson, A., & Hannah, M. C. (2016). A universal equation to predict methane production of forage-fed cattle in Australia. *Animal Production Science, 56*(3), 169-180. https://doi.org/10.1071/an15365

Costa, C. M., Difante, G. S., Costa, A. B. G., Gurgel, A. L. C., Ferreira, M. A., Jr, & Santos, G. T. (2021). Grazing intensity as a management strategy in tropical grasses for beef cattle production: a meta-analysis. *Animal, 15*(4), 100192. https://doi.org/10.1016/j.animal.2021.100192

Dias, C. S. A. M. M., Nunes, H. P. B., & Borba, A. E. S. (2023). Influence of the physical properties of samples in the use of NIRS to predict the chemical composition and gas production kinetic parameters of corn and grass silages. *Fermentation, 9*(5), 418. https://doi.org/10.3390/fermentation9050418

Erdaw, M. M. (2023). Contribution, prospects, and trends of livestock production in sub-Saharan Africa: a review. *International Journal of Agricultural Sustainability, 21*(1), 2247776. https://doi.org/10.1080/14735903.2023.2247776

Fakude, S. B., Soundy, P., & Sosibo, N. Z. (2025). Effect of selected factors on the prediction accuracy of plant-available phosphorus and potassium: A global meta-analysis for infrared spectroscopy protocol. *Agronomy, 15*(12), 2771. https://doi.org/10.3390/agronomy15122771

Gamon, J. A., Somers, B., Malenovský, Z., Middleton, E. M., Rascher, U., & Schaepman, M. E. (2019). Assessing vegetation function with imaging spectroscopy. *Surveys in Geophysics, 40*, 489-513. https://doi.org/10.1007/s10712-019-09511-5

Ghosh, S., & Sahu, T. N. (2023). Targeting zero hunger to ensure sustainable development: Insights from a panel structure. *Sustainable Development, 31*(4), 2814-2825. https://doi.org/10.1002/sd.2549

Hughes, M. P., Mlambo, V., Lallo, C. H. O., Basha, N. A. D., Nsahlai, I. V., & Jennings, P. G. A. (2017). Accuracy of two optical chlorophyll meters in predicting chemical composition and *in vitro* ruminal organic matter degradability of *Brachiaria* hybrid, *Megathyrsus maximus*, and *Paspalum atratum*. *Animal Nutrition, 3*(1), 67-76. https://doi.org/10.1016/j.aninu.2016.10.002

Jarque-Bascuñana, L., Bartolomé, J., Serrano, E., Espunyes, J., Garel, M., Calleja Alarcón, J. A., López-Olvera, J. R., & Albanell, E. (2021). Near infrared reflectance spectroscopy analysis to predict diet composition of a mountain ungulate species. *Animals, 11*(5), 1449. https://doi.org/10.3390/ani11051449

Kleen, J. L., & Guatteo, R. (2023). Precision livestock farming: What does it contain and what are the perspectives? *Animals, 13*(5), 779. https://doi.org/10.3390/ani13050779

Latimer, G. W. Jr. (Ed.). (2023). *Official Methods of Analysis of AOAC International. Association of Official Analytical Chemists*. https://doi.org/10.1093/9780197610145.002.001

Luo, X., Keenan, T. F., Chen, J. M., Croft, H., Prentice, I. C., Smith, N. G., Walker, A. P., Wang, H., Wang, R., Xu, C., & Zhang, Y. (2021). Global variation in the fraction of leaf nitrogen allocated to photosynthesis. *Nature Communications, 12*, 4866. https://doi.org/10.1038/s41467-021-25163-9

Monrroy, M., Gutiérrez, D., Miranda, M., Hernández, K., & García, J. R. (2017). Determination of *Brachiaria* spp. for-

age quality by near-infrared spectroscopy and partial least squares regression. *Journal of the Chilean Chemical Society, 62*(2), 3472-3477. https://doi.org/10.4067/s0717-97072017000200010

Namazzi, C., Sserumaga, J. P., Mugerwa, S., Kyalo, M., Mutai, C., Mwesigwa, R., Djikeng, A., & Ghimire, S. (2020). Genetic diversity and population structure of *Brachiaria* (syn. *Urochloa*) ecotypes from Uganda. *Agronomy, 10*(8), 1193. https://doi.org/10.3390/agronomy10081193

Parrini, S., Acciaioli, A., Crovetti, A., & Bozzi, R. (2018). Use of FT-NIRS for determination of chemical components and nutritional value of natural pasture. *Italian Journal of Animal Science, 17*(1), 87-91. https://doi.org/10.1080/1828051X.2017.1345659

Paul, N., Sunil, G. C., Horvath, D., & Sun, X. (2025). Deep learning for plant stress detection: A comprehensive review of technologies, challenges, and future directions. *Computers and Electronics in Agriculture, 229*, 109734. https://doi.org/10.1016/j.compag.2024.109734

Perry, L. A., Jassim, R. A., Gaughan, J. B., & Tomkins, N. W. (2017). Effect of feeding forage characteristic of wet- or dry-season tropical C4 grass in northern Australia, on methane production, intake and rumen outflow rates in *Bos indicus* steers. *Animal Production Science, 57*(10), 2033-2041. https://doi.org/10.1071/an15314

R Core Team. (2019). *The R Project for Statistical Computing*. https://www.r-project.org/

Radočaj, D., Plaščak, I., & Jurišić, M. (2023). Global navigation satellite systems as state-of-the-art solutions in precision agriculture: A review of studies indexed in the Web of Science. *Agriculture, 13*(7), 1417. https://doi.org/10.3390/agriculture13071417

Rao, I., Peters, M., Castro, A., Schultze-Kraft, R., White, D., Fisher, M., Miles, J., Lascano, C., Blummel, M., Bungenstab, D., Tapasco, J., Hyman, G., Bolliger, A., Paul, B., Van Der Hoek, R., Maass, B., Tiemann, T., Cuchillo, M., Douxchamps, S., Villanueva, C., Rincón, Á., Ayarza, M., Rosenstock, T., Subbarao, G., Arango, J., Cardoso, J., Worthington, M., Chirinda, N., Notenbaert, A., Jenet, A., Schmidt, A., Vivas, N., Lefroy, R., Fahrney, K., Guimarães, E., Tohme, J., Coo, S., Herrero, M., Chacón, M., Serchinger, T., & Rudel, T. (2015). LivestockPlus - The sustainable intensification of forage-based agricultural systems to improve livelihoods and ecosystem services in the tropics. *Tropical Grasslands-Forrajes Tropicales, 3*(2), 59-82. https://doi.org/10.17138/tgft(3)59-82

Robles-Zazueta, C. A., Pinto, F., Molero, G., Foulkes, M. J., Reynolds, M. P., & Murchie, E. H. (2022). Prediction of photosynthetic, biophysical, and biochemical traits in wheat canopies to reduce the phenotyping bottleneck. *Frontiers in Plant Science, 13*, 828451. https://doi.org/10.3389/fpls.2022.828451

Schindelin, J., Rueden, C. T., Hiner, M. C., & Eliceiri, K. W. (2015). The ImageJ ecosystem: An open platform for biomedical image analysis. *Molecular Reproduction and Development, 82*(7-8), 518-529. https://doi.org/10.1002/mrd.22489

Tan, P., Liu, H., Zhao, J., Gu, X., Wei, X., Zhang, X., Ma, N., Johnston, L. J., Bai, Y., Zhang, W., Nie, C., & Ma, X. (2021). Amino acids metabolism by rumen microorganisms: Nutrition and ecology strategies to reduce nitrogen emissions from the inside to the outside. *The Science of the Total Environment, 800*, 149596. https://doi.org/10.1016/j.scitotenv.2021.149596

Thomson, A. L., Humphries, D. J., Rymer, C., Archer, J. E., Grant, N. W., & Reynolds, C. K. (2018). Assessing the accuracy of current near infra-red reflectance spectroscopy analysis for fresh grass-clover mixture silages and development of new equations for this purpose. *Animal Feed Science and Technology, 239*, 94-106. https://doi.org/10.1016/j.anifeedsci.2018.03.009

Torres-Lugo, R. B., Solorio-Sánchez, F. J., Avilés, L. R. Y., Ku-Vera, J. C., Aguilar-Pérez, C. F., & Santillano-Cázares, J. (2022). Productivity, morphology and chemical composition of *Brachiaria* spp. ecotypes, under two solar illumination intensities, in Yucatan, Mexico. *Agronomy, 12*(11), 2634. https://doi.org/10.3390/agronomy12112634

Van Soest, P. J., Robertson, J. B., & Lewis, B. A. (1991). Methods for dietary fiber, neutral detergent fiber, and nonstarch polysaccharides in relation to animal nutrition. *Journal of Dairy Science, 74*(10), 3583-3597. https://doi.org/10.3168/jds.s0022-0302(91)78551-2

Xiong, D., Chen, J., Yu, T., Gao, W., Ling, X., Li, Y., Peng, S., & Huang, J. (2015). SPAD-based leaf nitrogen estimation is impacted by environmental factors and crop leaf characteristics. *Scientific Reports, 5*, 13389. https://doi.org/10.1038/srep13389

Zhao, Y., Zhao, Z., Shan, P., Peng, S., Yu, J., & Gao, S. (2019). Calibration transfer based on affine invariance for NIR without transfer standards. *Molecules, 24*(9), 1802. https://doi.org/10.3390/molecules24091802